TECHNIUM

Technium Vol. 3, Issue 1 pp.51-60 (2021)
ISSN: 2668-778X
www.techniumscience.com

Numerical Analysis and Simulationof RM12 turbofan rotor system

Hossein Rahmani[1]*, Amin Moslemi Petrudi [1], IonutCristian Scurtu [2]

[1] Department of Mechanical Engineering, IHUUniversity, Tehran, Iran

[2]Mircea cel Batran Naval Academy, Constanta, Romania

Email:*hsnrahmani@ihu.ac.ir*

Abstract: All rotating machines have vibrations and these vibrations have standard limits. The occurrence of various defects in the machines or non-observance of the permitted or standard values in repair works causes the amount of vibration to increase and consequently the parts to be damaged and cause irreparable damage. In this paper, the rotor and simulation of the rotor of a turbofan engine used in industry are investigated. The characteristics of this type of rotor are high performance, lightness, and low amplitude of vibrations. Various parameters such as rotational inertia, gyroscopic torque, rotational loading, the effects of mass imbalance, and instability in modeling have been investigated. Natural frequencies, critical velocity, and calculations have been used by Ansys software.The results of the numerical analysis and simulation were compared and there was a good agreement between these two modes of investigations, indicating the validity and accuracy of simulation assumptions.

Keywords: Vibrations, Instability, Numerical Analysis, Turbofan, Ansys software.

1. Introduction

Rotary or reciprocating shafts that are used to transmit force and torque and are affected by the torsional force and bending force and are divided into three groups: fixed, articulated, and bendable. Shafts are used to mount gears, clutches, belt wheels, and crankshafts. Crankshafts are also fixed shafts and are used to convert rotational to linear motion. Or vice versa. Joint shafts are rods whose angles are relative to each other and are used to transmit torsional forces between two shafts that are not in the same direction and are at different angles. The use of articulated shafts in milling machines, agricultural machines, transport machines, and cars. Rotating shafts are widely used in industry and are the main means of producing mechanical power transmission. Axes are the main components of steam, water, wind and gas turbines, generators and electric motors, combustion engines, pumps, compressors, fans, and all kinds of machine tools such as milling, stone turning, and drilling, ship propulsion, aircraft propellers, car wheels. And there are trains,etc. Axes are used in a wide range of dimensions and shapes from a few millimeters to a few meters and a weight of a few grams to several tons. Due to the importance of rotors in industry, a branch called rotor dynamics, which is a special branch of applied mechanics and studies the behavior and troubleshooting of the rotating mechanism. This branch of mechanics is used to analyze the behavior of jet engines, steam turbines, and pumps. In general, rotor dynamics studies a mechanical system consisting of a rotor mounted on bearings. The amplitude of vibrations of rotor-bearing systems is usually created and increased under the influence of humidity, and also, the discussion of instability in turbomachines leads to an increase in the amplitude of vibrations, which is related to its internal structure and must be corrected. Instability is a major concern for engineers designing large-scale rotors [1,2].

Some of the causes of vibration are:

- Non-axial components (couplings)
- Unbalance of car parts or improper use
- Lack of proper foundation for equipment installation
- Corrosion and wear of parts
- Loosen the bolts and nuts at their location
- Lack of proper operation of the device

Because unwanted vibrations are harmful in all structures and machines, it should be prevented by special measures. This issue is of special importance in rotating axes, which are investigated in the dynamic rotor. Axial vibrations can cause the system to fail both by causing severe vibrations, by applying large forces in the short term, and by causing mild vibrations and small forces in the long term due to fatigue. This type of failure can occur in shafts, blades, bearings, and even stators. Imbalance One of the common defects for rotating equipment is an imbalance. Improper and inhomogeneous distribution of mass in rotating objects is called imbalance. In other words, the imbalance is the accumulation and increase of mass in a part or parts of the body [3,4]. This accumulation can be due to the geometry of the object or due to its improper production. Imbalance occurs when the mass distribution is not symmetrical about the axis of rotation. In this case, the forces on one side of the axis will be more than the other directions. A piece that rotates around an axis of symmetry shows resistance to a change in this direction, called a gyroscopic effect. Important applications of the gyroscopic effect are in airplanes, ships, and space travel. The force of gyroscopic effects sometimes has to be considered in the design of machines. In most rotating systems, especially in vertical rotation systems, the shaft bears an axial force in addition to torsional torque transmission. The presence of tensile axial force increases the critical velocity. This increase is more pronounced on axes with low critical speeds. Instability is one of the important issues in the science of axial dynamics. Instability, in contrast to the resonance phenomenon that occurs at a certain speed, is observed in an area of the operating axis speed. When the rotational speed of the axis reaches the threshold of instability, the amplitude of the axis oscillations increases until nonlinear factors control the amplitude of the oscillations, while the phenomenon of damping intensification controls the amplitude of the oscillations [5,6]. Rahmani and Moslemi [7]. Analytical investigation of the vibrational and dynamic response of nano-composite cylindrical shell under thermal shock and mild heat field by DQM method. The vibrations and dynamic response of an orthotropic thin-walled composite cylindrical shell with epoxy graphite layers reinforced with carbon nanotubes under heat shock and heat field loading are investigated. The results show that increasing the outside temperature reduces the natural frequency and increases the displacement of the system. Radial displacement results were also compared with previous studies and were found to be in good agreement with previous literature. Increasing the percentage of carbon nanotubes also increased the natural frequency of the system and decreased the mobility of the middle layer. Scurtu and Moslemi et al [8]. Parametric optimization and calculation of vibrations introduced by propulsion installation. The mass of the shaft, the motor assembly, and the impeller are each examined as a centralized mass and are modeled by ANSYS software. Then, by extracting vibrational equations along the shaft axis and multi-objective optimization with response surface method (RSM). In this paper, the rotor and simulation of the rotor of a turbofan engine used in industry are investigated.

2. Statement of the problem

In this article, using finite element analysis, each of these four members is modeled and finally, the matrix related to each component is obtained, which is used to analyze the whole rotor set, the total mass matrix of the system, and the stiffness matrix of the whole system. The damping matrix of the whole system is assembled and placed in the following vibration equation, which will give the last equation after solving the system frequency response (Ehrlich, 1999).In the following equation, Ω is the rotational speed of the rotor.

$$[M]\{\ddot{\delta}\}+(\Omega[\mathrm{G}]+[\mathrm{C}])\{\dot{\delta}\}+[\mathrm{K}]\{\delta\}=\{\mathrm{f}\} \quad (1)$$

2.1Kinematics of rotating elements

A rotating element is considered as a rigid body and its rotational kinetic energy is calculated as follows:

$$T_{rot}=\frac{1}{2}(\mathrm{I}_{xx}\,\omega_x^{\,2}+I_{yy}\omega_y^{\,2}+I_{zz}\omega_z^{\,2}) \quad (2)$$

In general, the position of a rigid object in space by three angles α, β, Φ to Euler angles and a fixed coordinate system (bare) with fixed unit vectors and another with rotating unit vectors is a coordinate system on the center of a fixed rotating element Has been. When all of the Euler angles are zero, the two coordinate systems overlap. For a general position for the element in space, the connection between the two devices can be successfully and completely calculated in three steps with the mentioned Euler angles.

$$du_B^e = \frac{1}{2}\begin{Bmatrix} v' \\ w'' \end{Bmatrix}^T \begin{bmatrix} EI & 0 \\ 0 & EI \end{bmatrix} \begin{Bmatrix} v' \\ w'' \end{Bmatrix} ds \tag{3}$$

Which is *EI* flexural axis. If the element is also under a constant axial force, the strain energy stored in the disk will be called the strain energy under a constant axial load as follows:

$$du_A^e = -\frac{1}{2}\begin{Bmatrix} v' \\ w'' \end{Bmatrix}^T \begin{bmatrix} P & 0 \\ 0 & P \end{bmatrix} \begin{Bmatrix} v' \\ w'' \end{Bmatrix} ds \tag{4}$$

Strain energies for the whole element are obtained by integrating differential expressions over the entire length of the element:

$$U_A^e = \frac{EI}{2}\int_0^L \left[(\frac{\partial^2 u}{\partial y^2})^2 + (\frac{\partial^2 w}{\partial y^2})^2 \right] dy \tag{5}$$

$$U_A^e = \frac{F}{2}\int_0^L \left[(\frac{\partial u}{\partial y})^2 + (\frac{\partial w}{\partial y})^2 \right] dy \tag{6}$$

The total energy of the axis is obtained from Equation (7):

$$U_A^e = \frac{EI}{2}\int_0^L \left[(\frac{\partial^2 u}{\partial y^2})^2 + (\frac{\partial^2 w}{\partial y^2})^2 \right] dy + \frac{F}{2}\int_0^L \left[(\frac{\partial u}{\partial y})^2 + (\frac{\partial w}{\partial y})^2 \right] dy \tag{7}$$

The kinetic energy formula of an element uses the expansion of the disk kinetic energy equation located at a distance it is obtained from the length of the element (Xiang, 2011).

$$dT^e = \frac{1}{2}\begin{Bmatrix} v \\ w \end{Bmatrix}^T \begin{bmatrix} \mu & 0 \\ 0 & \mu \end{bmatrix} \begin{Bmatrix} v' \\ w'' \end{Bmatrix} ds + \frac{1}{2}\Phi \tau_p ds + \frac{1}{2}\begin{Bmatrix} \beta \\ \gamma \end{Bmatrix}^T \begin{bmatrix} I_d & 0 \\ 0 & I_d \end{bmatrix} \begin{Bmatrix} \beta \\ \gamma \end{Bmatrix} ds - \Phi \gamma \beta \tau_p ds \tag{8}$$

$$T_s = \frac{\rho s}{2}\int_0^L \left(\dot{u}^2 + \dot{w}^2 \right) dy + \frac{\rho l}{2}\int_0^L (\dot{\beta}^2 + \dot{\gamma}^2) dy + \rho I L \Omega^2 - 2\rho I \Omega \int_0^L \gamma \beta dy \tag{9}$$

By integrating the above expressions and applying Lagrange equations for the finite element, the shafts of the matrices are obtained (Nelson, 1980).

$$\left[M_T^e\right] = \frac{\rho AL}{420}\begin{bmatrix} 156 & 0 & 0 & 221 & 54 & 0 & 0 & -131 \\ 0 & 156 & -221 & 0 & 0 & 54 & 131 & 0 \\ 0 & -221 & 4l^2 & 0 & 0 & -131 & -3l^2 & 0 \\ 221 & 0 & 0 & 4l^2 & 131 & 0 & 0 & -3l^2 \\ 54 & 0 & 0 & 131 & 156 & 0 & 0 & -221 \\ 0 & 54 & -131 & 0 & 0 & 156 & 221 & 0 \\ 0 & 131 & -3l^2 & 0 & 0 & 221 & 4l^2 & 0 \\ -131 & 0 & 0 & -3l^2 & -221 & 0 & 0 & 4l^2 \end{bmatrix} \tag{10}$$

$$\left[K_T^e\right]=\frac{E\times l}{L^3}\begin{bmatrix} 12 & 0 & 0 & 6L & -12 & 0 & 0 & 6L \\ 0 & 12 & -6L & 0 & 0 & -12 & -6L & 0 \\ 0 & -6L & 4l^2 & 0 & 0 & 6L & 2l^2 & 0 \\ 6l & 0 & 0 & 4l^2 & -6L & 0 & 0 & 2l^2 \\ -12 & 0 & 0 & -6L & 12 & 0 & 0 & -6L \\ 0 & -12 & 6L & 0 & 0 & 12 & 6L & 0 \\ 0 & -6L & 2l^2 & 0 & 0 & 6L & 4l^2 & 0 \\ 6L & 0 & 0 & 2l^2 & -6L & 0 & 0 & 4L^2 \end{bmatrix} \tag{11}$$

$$\left[K_A^e\right]=\frac{F}{30L}\begin{bmatrix} 36 & 0 & 0 & 3L & -36 & 0 & 0 & 3L \\ 0 & 36 & -3L & 0 & 0 & -36 & -3L & 0 \\ 0 & -3L & 4L^2 & 0 & 0 & 3L & -L^2 & 0 \\ 3L & 0 & 0 & 4L^2 & -3L & 0 & 0 & -L^2 \\ -36 & 0 & 0 & -3L & 36 & 0 & 0 & -3L \\ 0 & -36 & 3L & 0 & 0 & 36 & 3L & 0 \\ 0 & -3L & -L^2 & 0 & 0 & 3L & 4L^2 & 0 \\ 3L & 0 & 0 & -L^2 & -3L & 0 & 0 & 4L^2 \end{bmatrix} \tag{12}$$

$$\left[M_R^e\right]=\frac{\mu r^3}{120l}\begin{bmatrix} 36 & 0 & 0 & 3L & -36 & 0 & 0 & 3L \\ 0 & 36 & -3L & 0 & 0 & -36 & -3L & 0 \\ 0 & -3L & 4L^2 & 0 & 0 & 3L & -L^2 & 0 \\ 3L & 0 & 0 & 4L^2 & -3L & 0 & 0 & -L^2 \\ -36 & 0 & 0 & -3L & 36 & 0 & 0 & -3L \\ 0 & -36 & 3L & 0 & 0 & 36 & 3L & 0 \\ 0 & -3L & -L^2 & 0 & 0 & 3L & 4L^2 & 0 \\ 3L & 0 & 0 & -L^2 & -3L & 0 & 0 & 4L^2 \end{bmatrix} \tag{13}$$

$$\left[G_R^e\right]=\frac{2\mu r^3}{120l}\begin{bmatrix} 0 & -36 & 3L & 0 & 0 & 36 & 3L & 0 \\ 36 & 0 & 0 & 3L & -36 & 0 & -3L & 3L \\ -3L & 0 & 0 & -4L^2 & 3L & 0 & -L^2 & L^2 \\ 0 & -3L & 4L^2 & 0 & 0 & 3L & 0 & 0 \\ 0 & 36 & -3L & 0 & 0 & -36 & 0 & 0 \\ -36 & 0 & 0 & -3L & 36 & 0 & 3L & -3L \\ -3L & 0 & 0 & L^2 & 3L & 0 & 4L^2 & 0 \\ 0 & -3L & -L^2 & 0 & 0 & 3L & 0 & 4L^2 \end{bmatrix} \tag{14}$$

3. Simulation of RM12 turbofan rotor system

The turbofan engine selected in this article will be used in the Saab JAS 39 Gripe fighter. The working speed of this rotor is 30000 RPM (3140 radians per second). The general view of the turbine and the parts that are important in vibrations are shown below. This turbofan engine consists of three fan stages, seven axial compressor stages, one low-pressure turbine stage, and one high-pressure turbine stage with a shaft connected between them. The rotor is mounted on four bearings whose positions are marked. The components of the rotor are turbines and shafts, respectively, which are made of steel alloys, the compressor is made of aluminum alloys, and the fan used is made of titanium.Table 1 shows the specifications of materials used in the rotor and, Table 2 shows the weight of parts used in the gas turbine rotor.

Table 1. Specifications of materials used in the rotor.

Mechanical properties	Steel	Aluminum	Titanium
Young modulus (GPa)	207	71	116
Shear modulus (GPa)	80	26	44
Poisson's ratio	0.3	0.35	0.35
Volumetric mass (kg/m3)	7800	2700	4506
Thermal expansion coefficient (1/C)	14×10^{6}	23×10^{6}	8.6×10^{6}

Table 2. Weight of parts used in the gas turbine rotor.

Name	Material	Unit weight (kg)	Number	The total weight (kg)
Low-pressure steel turbine	Steel	25.11	1	25.11
High-pressure steel turbine	Steel	11.78	1	11.78
High-pressure compressor	Steel + Aluminum	18.31	1	18.31
Fan set	Steel + Titanium	29.13	1	29.13
The whole set of rotors	-	-	-	139.68

All turbofan rotor parts have been modeled in Katia software after measuring dimensions in millimeters and finally, the assembly has been disassembled. Fig 1 shows the turbofan rotor finite element model. in.Fig 2 shows the complete model of the RM12 rotor. The main model of turbofan with blades is shown in Fig 3.

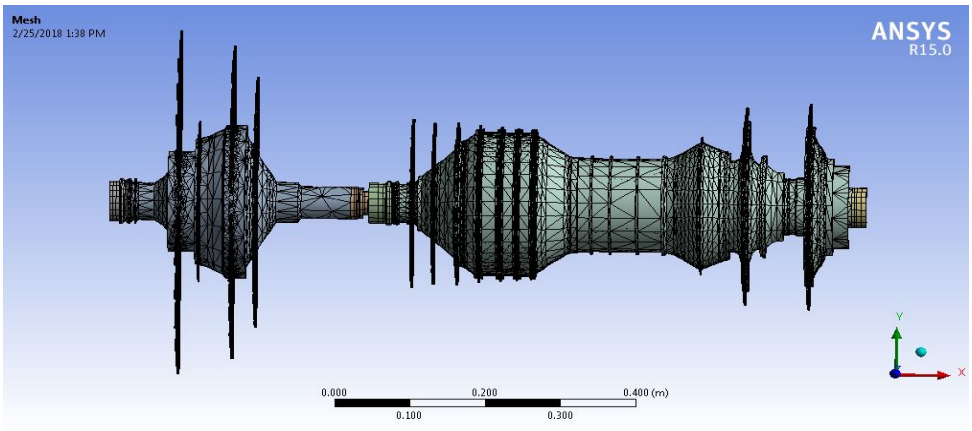

Fig. 1. Turbofan rotor finite element model.

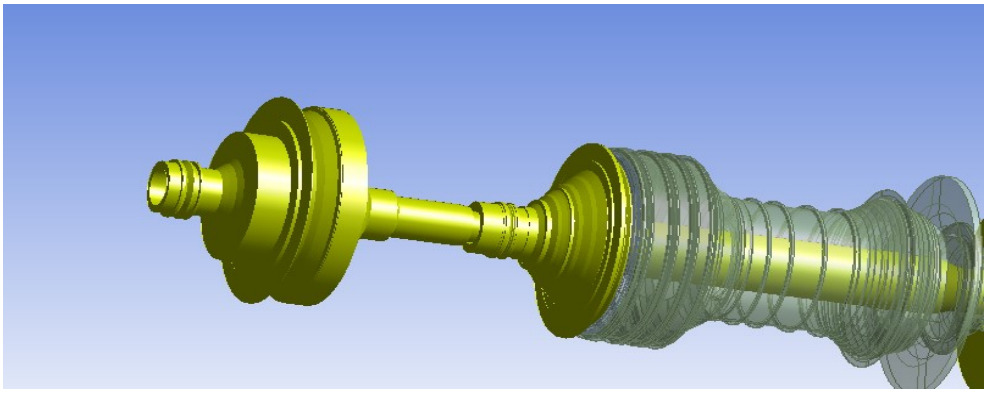

Fig. 2. The complete model of the RM12 rotor.

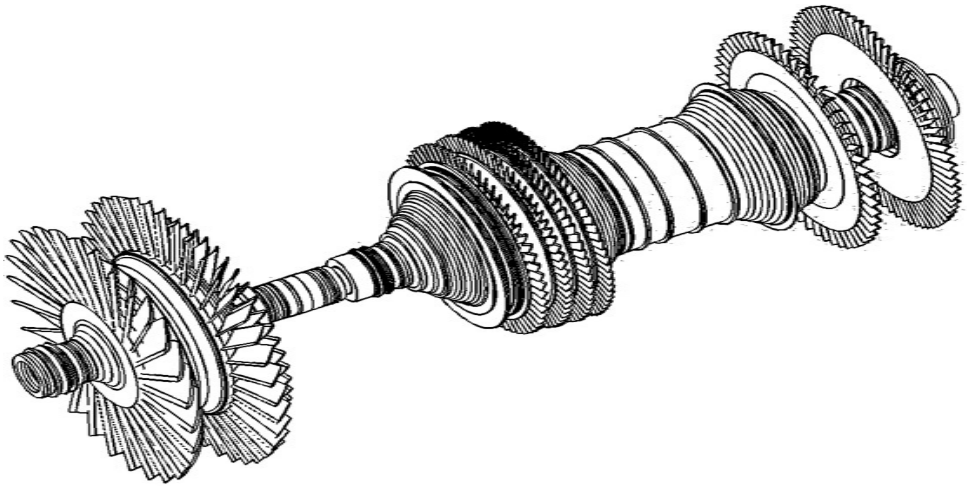

Fig. 3. Turbofan RM12 model.

3.1.RM12 rotor with roller bearing

To use the roller bearing in the RM12 rotor, the stiffness parameters of this bearing can be defined as follows: The location of the bearings is as shown in Fig 4.

$$K_{11} = 1\times10^{7}$$
$$K_{22} = 1\times10^{7}$$
$$K_{12} = 2\times10^{6} \quad (15)$$
$$K_{21} = 2\times10^{6}$$

The bearings are shown in the locations shown in the figure. In this bearing, the rotational movement in the direction of the axis is restricted. The lame frequencies along with the critical speed for a rotor with rigid bearings are shown in Table 3. Fig 4 shows a Campbell RM12 rotor diagram with a roller bearing in the applied frequency range. Figs 5-10 shows the RM12 rotor modes of a roller bearing.Fig 11 shows the harmonic response of RM12 rotor with roller bearing to unbalance mass.

Table 3. Results from the Ansys rotor program with roller bearings.

Ansys results (Hz frequency)	Critical velocity (Hz)	Mode number
1288	1419.42	1FW
1348	1396.88	2BW
1392	1410.83	3BW
1455	1487.9	4BW
1573	1599.56	5BW
1605	1678.09	6BW
1758	1766.91	7FW
1778	1723.47	8BW
1945	1942.19	9BW
2002	2109.1	10FW
2382	2313.69	11FW

Technium Vol. 3, Issue 1 pp.51-60 (2021)
ISSN: 2668-778X
www.techniumscience.com

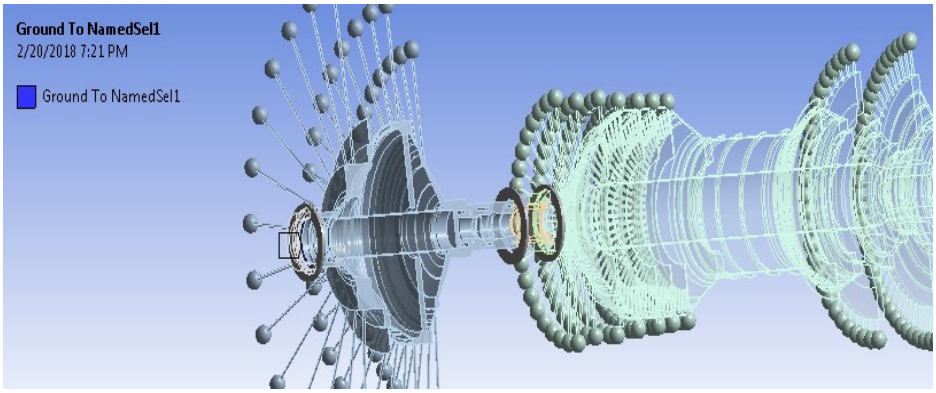

Fig. 4. RM12 rotor with roller bearing.

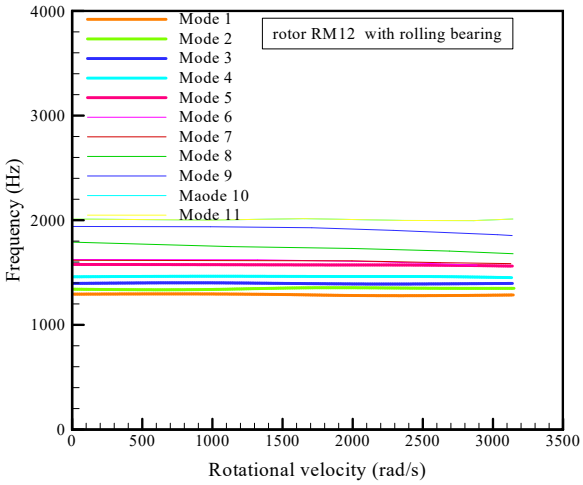

Fig. 4. Campbell rotor diagram with roller bearing.

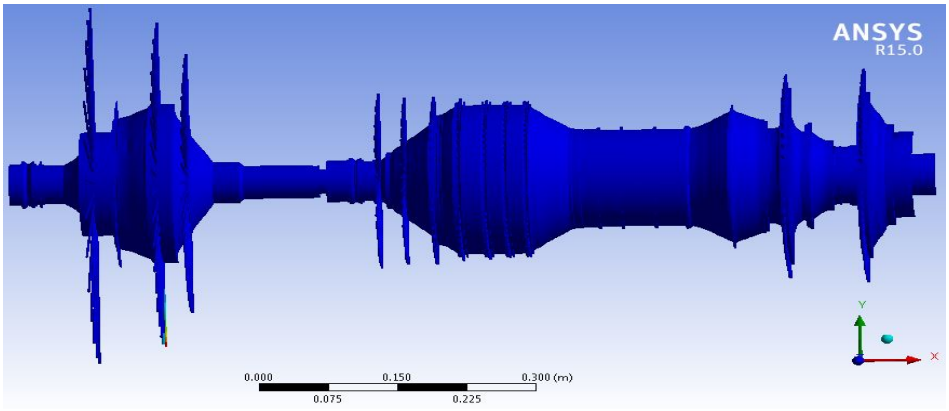

Fig. 5. The first mode (torsion) of the rotor.

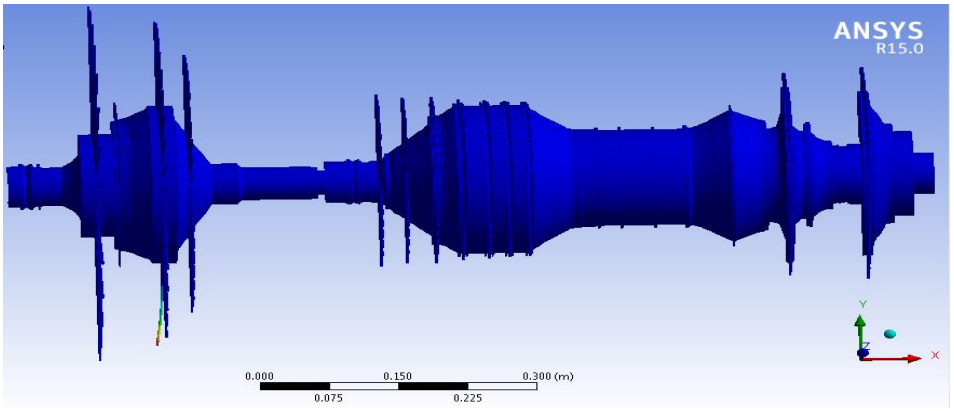

Fig. 6. The second mode (bending) of the rotor.

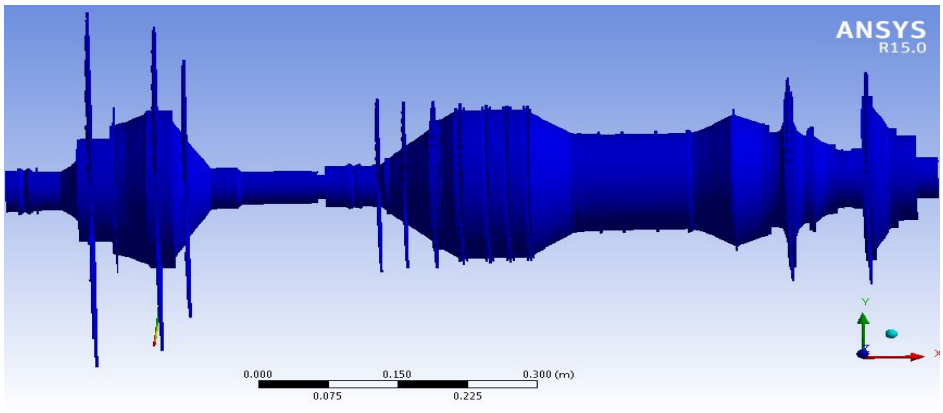

Fig. 7. The third mode (bending) of the rotor.

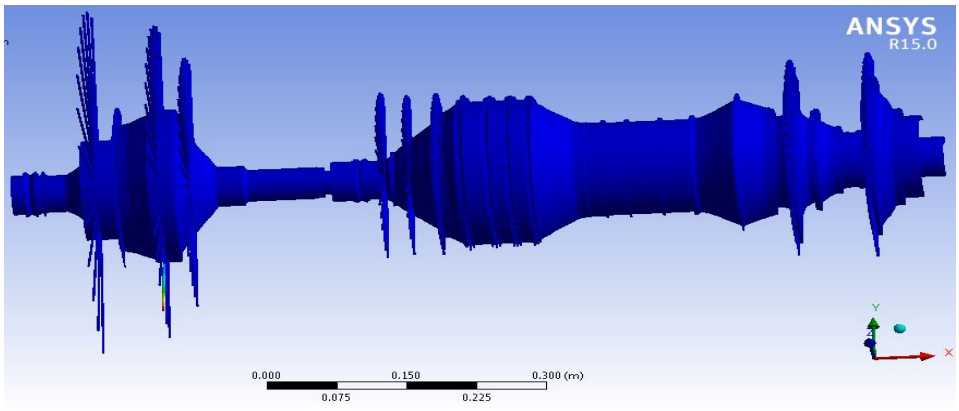

Fig. 8. Fourth (torsional) mode of the rotor.

Technium Vol. 3, Issue 1 pp.51-60 (2021)
ISSN: 2668-778X
www.techniumscience.com

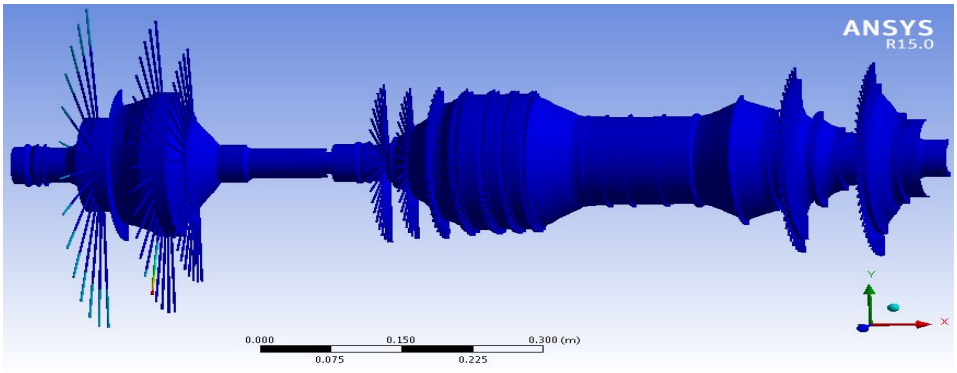

Fig. 9. Fifth (torsional) mode of the rotor.

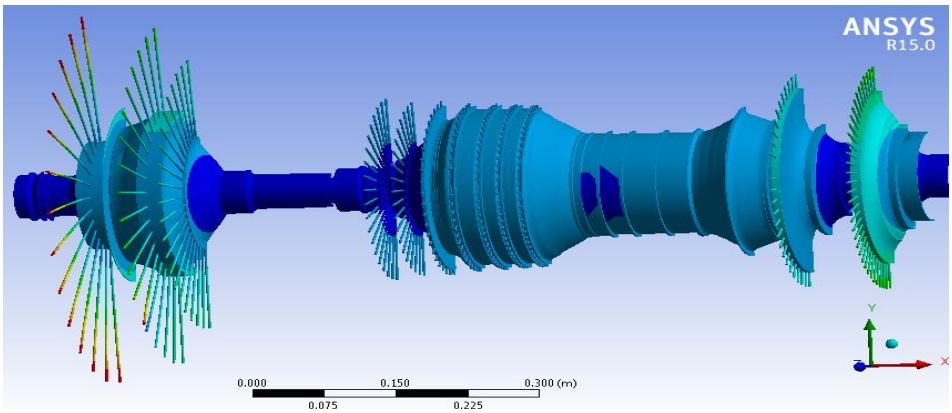

Fig. 10. Sixth (torsional) mode of the RM12 rotor.

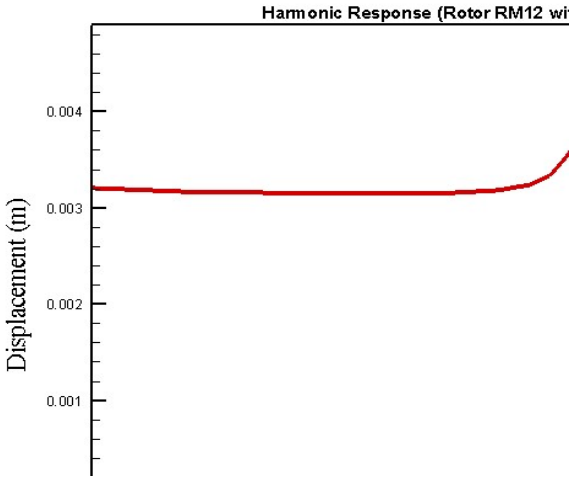

Fig. 11. The harmonic response of RM12 rotor with roller bearing to unbalance mass.

4. Conclusion

The main frequencies of the rotor were calculated at the specified rotational speed, the results of which are fully specified.Due to the shape of the modes obtained in each case, the most displacement has occurred in the RM12 rotor fan, so reducing the vibrations of the input fan to prevent failure, should be considered as an important parameter.In rolling bearing, the slip of the motion threshold is twice that of the slip. But this amount of friction compared to sleeve bearings can be ignored. Oil load, velocity, and viscosity are factors that affect the friction characteristics of rolling bearings. Bearings are designed to withstand a net radial load, a net load thrust, or a combination of the two. The figure below shows the different parts of a roller bearing. The results of the numerical analysis and simulation were compared and there was a good agreement between these two modes of investigations, indicating the validity and accuracy of simulation assumptions.

References

[1] Eshleman, R., L., and Eubanks, R. A., 1969," On the Critical Speeds of a Continuous Rotor" , Journal of Engineering for Industry, Trans. Of the ASME, Vol.91, P.1180.

[2] Chen,L. W., Sheu, H.C., 1998," Stability Behavior of a Shaft-Disk System Subjected to Longitudinal Force" Journal of Propulsion and Power,Vol.14, P.357-383

[3] Loewy, R.G., and Piarulli, V.J., 1969, "Dynamics of Rotating shaft, The shock and Vibration Information Center Naval Research Laboratory", Washington D.C.

[4] Bolotin, V.V., 1963," Nonconservative Problems of the Theory of Elastic stability", pergamon, Oxford.

[5] Gasch,R., 1993,"A Survey of the Dynamic Behavior of aSimple Rotating Shaft With a Transverse Crack",Journal of sound and Vibration, vol. 160,P.213

[6] Khader,N., 1997,"Stability Analysis for the Dynamic Dynamics Design of Rotor", Journal of Sound and Vibration, Vol, P.287

[7] Rahmani, M., & Petrudi, A. M. (2020). Analytical Investigation of the Vibrational and Dynamic Response of Nano-Composite Cylindrical Shell Under Thermal Shock and Mild Heat Field by DQM Method. Journal of Modeling and Simulation of Materials, 3(1), 22-36.

[8] Scurtu, I. C., Petrudi, A. M., & Rahmani, M. (2020, December). 2. Parametric optimization and calculation of vibrations introducted by propulsion installation. In Proceedings Of International Conference Building Services And Energy Efficiency (pp. 15-28). Sciendo.